Computation of Electromagnetic Waves Diffraction by Spectral Moments Method

Driss Chenouni, Zakia Lakhliai, Claude Benoit, Gérard Poussigue, and Abdallah Sakout

***Abstract*— In this paper, we solve, for the first time, electromagnetic wave propagation equations in heterogeneous media using the spectral moments method. This numerical method, first developed in condensed matter physics, was recently successfully applied to acoustic waves propagation simulation in geophysics. The method requires the introduction of an auxiliary density function, which can be calculated by the moments technique. This allows computation of the Green's function of the whole system as a continued fraction in time Fourier domain. The coefficients of the continued fraction are computed directly from the dynamics matrix obtained by discretization of wave propagation equations and from the sources and receivers. We illustrate this method through the study of a plane wave diffraction by a slit in two-dimensional (2-D) media and by a rectangular aperture in three-dimensional (3-D) media. Comparison with analytical results obtained with the Kirchhoff theory shows that this method is a very powerful tool to solve propagation equations in heterogeneous media. Last, we present a brief comparison with other computing methods.**

I. Introduction

MODELING wave propagation in heterogeneous media requires the development of high-performance numerical algorithms. Over the past several years, many modeling techniques have been proposed to solve Maxwell's equations. Finite-element and finite-difference methods can be used as references to model electromagnetic scattering problems [1]. In all these methods, absorbing boundary conditions play a key role: several techniques were recently proposed to solve these problems [2]–[4]. We could also mention the so-called "moment of methods" (MoM) [5], [6]. These latter methods involve inversion of large full matrices, limiting the discretization fineness of the system under consideration. In this paper, we present the application of a method called the "spectral moments method" to electromagnetic wave propagation simulation in heterogeneous media. This method is based on determination of the exact Green functions of the system. For all frequencies, the system response (electric or magnetic field) to a given source is obtained from the Green functions. Direct determination of the Green functions requires computation of all eigenvalues and eigenvectors of matrices limiting the size of these matrices. These difficulties can be avoided by using the spectral moments method (SMM), which allows management of very large matrices. Indeed, in the MoM, the matrices are full and their dimensions are usually about (2000 to 4000 $\times$ 2000 to 4000). In the SMM the matrices are sparse and we are now able to deal matrices (20 000 000 $\times$ 20 000 000). Of course, in the examples presented in the paper, the part of the discretization grid occupied by source, slit and receiver is very small. But, in other diffraction simulations this part is greater and, with the introduction of absorbing boundary conditions, it may reach a few percents.

For harmonic solids, the moments method was first introduced by Montroll [7] to calculate the density of one-phonon state and was improved by Blumstein and Wheeler [8] and Wheeler [9]. In the dynamics of condensed matter, the exact evaluation of the response was developed by Benoit [10], [11] and applied to the study of fractals as the Sierpinski's gasket by Benoit [12], percolating networks by Royer [13], [14], silica aerogels by Rahmani [15], [16], dynamical properties of polymers by Poussigue [17], quasi-crystals by Benoit [18] and Poussigue [19], and to damped systems by Benoit [20]. In solid-state physics, the moments method has been developed to study electronic properties by Gaspard and Cyrot-Lackmann [21], Lambin and Gaspard [22], Turchi [23] and Jurczek [24]. These methods are mathematically equivalent to Lanczos [25] or the recursion procedure of Haydock [26] and, in many aspects, Jurczek [24] and Benoit [27]. In fact, the moments method is much more general than the Lanczos procedure and was solved by Stieltjes [28]. The spectral moments method was recently successfully applied to the propagation simulation of acoustic waves in geophysics by Rousseau [29]. The first application of this method to the electromagnetic waves propagation simulation in anisotropic media was presented in Benoit [30].

In this paper, we first present the general propagation equations. Then, the main features of SMM are described along with the procedure to compute Green functions. In the last section, SMM is applied to the simulation of wave propagation in two-dimensional (2-D) and in three-dimensional (3-D) heterogeneous media.

II. Motion Equations

In macroscopic form, electromagnetic waves satisfy the following Maxwell's equations [31]:

$$\frac{\partial \vec{D}}{\partial t} - \vec{\nabla} \times \vec{H} = -\vec{J}_0(\vec{r}, t) \tag{1}$$

Manuscript received September 20, 1995; revised February 24, 1997.

D. Chenouni and A. Sakout are with the Laboratoire d'Optique et de Spectroscopie, Faculté des Sciences—Dhar El Mehraz, Atlas-Fes, BP 1796 Morocco.

Z. Lakhliai is with the Ecole Superieure de Technologie de Fes, Fes, BP 2427 Morocco.

C. Benoit and G. Poussigue are with the Groupe de Dynamique des Phases Condensées UMR 5581, Université de Montpellier II, Place Eugène Bataillon, Montpellier Cedex 5, 34095 France.

Publisher Item Identifier S 0018-926X(98)01484-7.

and

$$\vec{\nabla}\cdot\vec{D}=\rho_0(\vec{r},t) \tag{2}$$

where $\rho_0(\vec{r},t)$ and $\vec{J_0}(\vec{r},t)$ are, respectively, the free charges and current density. With time-harmonic fields, we can write directly

$$\vec{D}=[\varepsilon]\vec{E} \tag{3}$$

and

$$\vec{B}=[\mu]\vec{H} \tag{4}$$

where $[\varepsilon]$ and $[\mu]$ represent dielectric and permeability tensors, respectively. In this work, we assume that the media are isotropic and heterogeneous so that $[\varepsilon]$ and $[\mu]$ are diagonal 3×3 tensors depending on spatial coordinates and frequency ω.

Introducing the vector potential $\vec{A}(\vec{r},t)$ and the scalar potential $V(\vec{r},t)$, we find that the vector potential satisfies the inhomogeneous wave equation

$$\nabla\vec{A}+\mu(r)\vec{\nabla}\mu^{-1}(r)(\vec{\nabla}\vec{A})-\mu(r)\vec{\nabla}\mu^{-1}(r)\times(\vec{\nabla}\times\vec{A})-\varepsilon^{-1}(r)(\vec{\nabla}\vec{A})\vec{\nabla}\varepsilon(r)-\mu(r)\varepsilon(r)\frac{\partial^2\vec{A}}{\partial^2 t}=-\mu(r)\vec{J}_0. \tag{5}$$

Now, if we are dealing with nonferromagnetic material, we can assume that permeability is constant. Thus, (5) becomes

$$\nabla\vec{A}-\varepsilon^{-1}(r)\vec{\nabla}\varepsilon(r)\vec{\nabla}\cdot\vec{A}-\mu\varepsilon(r)\frac{\partial^2\vec{A}}{\partial^2 t}=-\mu\vec{J}_0. \tag{6}$$

The scalar potential will be obtained from the Lorentz relation. It is very convenient to introduce a discrete base or site representation. Let us consider the vector field $\vec{u}(\vec{r},t)$ taking the value $\vec{u}(\vec{r}_n,t)=\vec{u}(n,t)$ in point $\vec{r}_n$, we introduce in Dirac notation the column vector $|U\rangle$ of the discrete space such that

$$|U(t)\rangle=\sum_{\alpha n}u_\alpha(n,t)|\alpha n\rangle. \tag{7}$$

$|\alpha n\rangle$ is the base in the real space or site representation, with $\alpha,\beta=(x,y,z)$. This base is assumed to be orthogonal and complete

$$\langle\alpha n\mid\beta n'\rangle=\delta_{\alpha\beta}\delta_{nn'}\quad\text{and}\quad\sum_{\alpha n}|\alpha n\rangle\langle\alpha n|=I. \tag{8}$$

$|\alpha n\rangle$ is equivalent to $\vec{e}_\alpha(n)$ a vector of the canonical base. $\vec{e}_\alpha$ is a three component vector (for the three components of the vector potential) at every site n of the lattice.

In a discrete space, using the finite-difference scheme, (6) leads to the motion equation

$$\frac{\partial^2|\bar{A}\rangle}{\partial t'^2}=-\mathbf{D}|\bar{A}\rangle-|\bar{J}\rangle \tag{9}$$

with $t'=ct$, $\bar{A}_\alpha(n)=\sqrt{\varepsilon_r(n)\mu_r}A_\alpha(n)$ and

$$\langle\alpha n\mid\bar{J}\rangle=\bar{J}_{0\alpha}(n)=-\sqrt{\frac{\mu_r}{\varepsilon(n)}}\mu_0 J_{0\alpha}(n). \tag{10}$$

In heterogeneous media, it is necessary to take into account the gradient term in (6). Then matrix $\mathbf{D}$ is sometimes nonsymmetrical. Its elements are given by

$$\begin{aligned}D_{\alpha\beta}(n,n')=&\left(2\delta_{nn'}-\delta_{nn'+1_{(\alpha)}}-\delta_{nn'-1_{(\alpha)}}\right)\\&\times\delta_{\alpha\beta}\frac{1}{\Delta\alpha^2}\frac{1}{\sqrt{\varepsilon_r(n)\mu_r\varepsilon_r(n')\mu_r}}\\&+\left(\delta_{nn'-1_{(\beta)}}-\delta_{nn'+1_{(\beta)}}\right)\left(\varepsilon_r\left(n+1_{(\alpha)}\right)\right.\\&\left.-\varepsilon_r\left(n-1_{(\alpha)}\right)\right)\frac{1}{4\Delta\alpha\Delta\beta}\frac{1}{\sqrt{\varepsilon_r^3(n)\mu_r\varepsilon_r(n')\mu_r}}\end{aligned} \tag{11}$$

where $\pm 1_{(\alpha)}$ indicates a displacement of one step in the lattice in the α direction. $\Delta\alpha$ is the nodal interval in the α direction.

To solve (9), we introduce the Green matrix which satisfies

$$\ddot{\mathbf{G}}(t-t')+\mathbf{D}\mathbf{G}(t-t')=-\mathbf{I}\delta(t-t'). \tag{12}$$

Usually $\mathbf{G}(t-t')$ is subject to certain boundary conditions. These conditions have been taken into account in the evaluation of matrix $\mathbf{D}$. They can be described in such a way—if in (11) n' is outside the discretized box, then it is replaced by $n'_T=n'\pm N\alpha_{(\alpha)}$ ($N\alpha$ being the dimension of the lattice in the α direction) in such a way that n'_T is inside the box. Then $D_{\alpha\beta}(n,n'_T)$ is equal to $D_{\alpha\beta}(n,n')$ (periodical boundary conditions) or $D_{\alpha\beta}(n,n'_T)$ is equal to zero (free boundary conditions).

Formally, the solution of (9) is given by

$$|\bar{A}(t)\rangle=\int\mathbf{G}(t-t')|\bar{J}(t')\rangle\,dt' \tag{13}$$

so the Green matrix allows us to compute the response function. Now, If we want to work with the electromagnetic field with the help of

$$[\varepsilon(r)\mu]^{-\frac{1}{2}}=\frac{1}{\sqrt{\varepsilon_0\mu_0}}[\varepsilon_r(r)\mu_r]^{-\frac{1}{2}}=c[\varepsilon_r(r)\mu_r]^{-\frac{1}{2}} \tag{14}$$

and

$$\vec{E}'=[\varepsilon_r(r)\mu_r]^{\frac{1}{2}}\vec{E} \tag{15}$$

(1) becomes

$$\frac{\partial\vec{E}'}{\partial(ct)}=[\varepsilon_r(r)\mu_r]^{-\frac{1}{2}}(\vec{\nabla}\times(c\vec{B})-c\mu_0[\varepsilon_r(r)]^{-\frac{1}{2}}(\mu_r)^{\frac{1}{2}}\vec{J}_0. \tag{16}$$

Now, with $\vec{B}'=c\vec{B}$, $t'=ct$, and $\mu_r=1$ (nonmagnetic materials), one obtains the following equations:

$$\frac{\partial\vec{E}'}{\partial t'}=[\varepsilon_r(r)]^{-\frac{1}{2}}\vec{\nabla}\times\vec{B}'-\vec{J}'\quad\text{with }\vec{J}'=c\mu_0[\varepsilon_r(r)]^{-\frac{1}{2}}\vec{J}_0 \tag{17}$$

and

$$\frac{\partial\vec{B}'}{\partial t'}=-\vec{\nabla}\times\left([\varepsilon_r(r)]^{-\frac{1}{2}}\vec{E}'\right). \tag{18}$$

The space discretization of (17) and (18), using the finite-difference scheme, leads to the following motion equation:

$$\frac{d}{dt'}\begin{pmatrix} E'_x(1)\\ E'_y(1)\\ E'_z(1)\\ B'_x(1)\\ \cdot\\ E'_x(n)\\ E'_y(n)\\ E'_z(n)\\ B'_x(n)\\ B'_y(n)\\ B'_z(n)\\ \cdot\\ \cdot\\ \cdot\\ B'_z(N)\end{pmatrix} = -\mathbf{M}\begin{pmatrix} E'_x(1)\\ E'_y(1)\\ E'_z(1)\\ B'_x(1)\\ \cdot\\ E'_x(n)\\ E'_y(n)\\ E'_z(n)\\ B'_x(n)\\ B'_y(n)\\ B'_z(n)\\ \cdot\\ \cdot\\ \cdot\\ B'_z(N)\end{pmatrix} - \begin{pmatrix} J'_x(1)\\ J'_y(1)\\ J'_z(1)\\ \cdot\\ \cdot\\ J'_x(n)\\ J'_y(n)\\ J'_z(n)\\ \\ \\ \\ \cdot\\ \cdot\\ \cdot\\ \cdot\end{pmatrix} \tag{19}$$

which can be written in matrix form

$$\frac{d|\Phi\rangle}{dt'} = -\mathbf{M}|\Phi\rangle - |J'\rangle. \tag{20}$$

The vector $|\Phi\rangle$ is given by

$$\langle \alpha n \mid \Phi\rangle = \Phi_\alpha(n) \tag{21}$$

where

$$\Phi_\alpha(n) = E'_\alpha(n), \qquad \text{if } \alpha = 1,2,3 \quad (1=x, 2=y, 3=z) \tag{22}$$

and

$$\Phi_\alpha(n) = B'_\alpha(n), \qquad \text{if } \alpha = 4,5,6 \quad (4=x, 5=y, 6=z) \tag{23}$$

$\langle \alpha n \mid J'\rangle = J'_\alpha(n)$ here represents a current density source. $|\alpha n\rangle$ is equivalent to $\vec{e_\alpha}(n)$ a vector of the canonical base. Now, $\vec{e_\alpha}$ is a six component vector (for the three components of the electric field and the three components of the magnetic field) at every site n of the lattice.

Matrix $\mathbf{M}$ is anti-symmetrical even under heterogeneous conditions. As for the field potentials, we introduce the Green matrix given now by

$$\dot{\mathbf{G}}(t-t') + \mathbf{M}\mathbf{G}(t-t') = -\mathbf{I}\delta(t-t'). \tag{24}$$

The solution of (20) is given by

$$|\Phi(t)\rangle = \int \mathbf{G}(t-t')|J'(t')\rangle\, dt'. \tag{25}$$

We now show how to calculate the Green matrix with SMM. The mathematical aspect of this method has been developed in previous papers [20], [27], [30], so we will just recall the main points concerning application to electromagnetic wave propagation.

III. The Spectral Moments Method

A. Method

Physical properties must not depend on the time origin, so the Green matrix is only a function of the time interval $t-t'$. So it is very convenient to work with the time Fourier domain. Finally, the time dependence of the electromagnetic field will be obtained, if it is necessary, by using the inverse Fourier transform. So, introducing the Fourier transform $\mathbf{G}(\omega)$ of $\mathbf{G}(t-t')$

$$\mathbf{G}(t-t') = \frac{1}{2\pi}\int \mathbf{G}(\omega)e^{-i\omega(t-t')}\, d\omega \tag{26}$$

the response to an external source is given by

$$|\psi(\omega)\rangle = \mathbf{G}(\omega)|F(\omega)\rangle \tag{27}$$

which can be expressed in terms of components, using relations (8) and (27)

$$\langle \alpha n \mid \psi(\omega)\rangle = \sum_{\beta n'}\langle \alpha n|\mathbf{G}(\omega)|\beta n'\rangle\langle \beta n' \mid F(\omega)\rangle \tag{28}$$

with $|\psi(\omega)\rangle = |A(\omega)\rangle$ if we work with vector potential or $|\psi(\omega)\rangle = |\Phi(\omega)\rangle$ if we work with electromagnetic fields. Let us recall that

$$\langle \alpha n|\mathbf{G}(\omega)|\beta n'\rangle = G_{\alpha\beta}(n,n',\omega) \tag{29}$$

and

$$\langle \alpha n \mid F(\omega)\rangle = F_\alpha(n,\omega). \tag{30}$$

The Fourier transform of the Green matrix is given by

$$\mathbf{G}(\omega) = -((-i\omega)^m\mathbf{I} + \mathbf{K})^{-1} \tag{31}$$

where $m = 1$ and $\mathbf{K} = \mathbf{M}$ with the $(\vec{E}, \vec{B})$ fields and $m = 2, \mathbf{K} = \mathbf{D}$ with the $\vec{A}$ field. From (28) and (31), we see that determination of the response function $\langle \alpha n \mid \psi(\omega)\rangle$ involves determination of the matrix element

$$\langle \alpha n|\mathbf{G}(\omega)|\beta n'\rangle = -\langle \alpha n|((-i\omega)^m\mathbf{I} + \mathbf{K})^{-1}|\beta n'\rangle. \tag{32}$$

We see that $((-i\omega)^m\mathbf{I} + \mathbf{K})^{-1}$ exists only if $-(-i\omega)^m$ differs from the eigenvalues of matrix $\mathbf{K}$. The difficulty is avoided by adding an imaginary part ε such that $\varepsilon \to 0+$.

With the $\vec{A}$ field, we introduce the variable $z = \omega^2 + i\varepsilon = u + i\varepsilon$, while with the $(\vec{E}, \vec{B})$ fields we introduce $z = i(\omega + i\varepsilon)$. In the absence of absorption, eigenvalues of the $\mathbf{D}$ matrix are strictly real while eigenvalues of the $\mathbf{M}$ matrix are purely imaginary. Introduction of the coefficient ε is the same as introducing a dissipation mechanism in the media. This effect will play a key role afterwards. We call $\lambda_j = \omega_j^2$ and $\mu_j = i\mu'_j$ the eigenvalues of $\mathbf{D}$ and $\mathbf{M}$ matrices, respectively.

Let us now present the main features of SMM which are detailed in Benoit [20], [27], [30] and Royer [32].

Determination of the response function involves computation of the nondiagonal element (32). Introducing the eigenvalues and the left and right eigenvectors of the matrix $\mathbf{K}$

$$\mathbf{K}|j\rangle_R = \eta_j|j\rangle_R \tag{33}$$

$$_L\langle j|\mathbf{K} = {}_L\langle j|\theta_j \tag{34}$$

where $\eta_j = \mu_j$ or λ_j with $m = 1$ or 2. $|j\rangle_R$ and $|j\rangle_L$ are the right and left eigenvectors of matrix $\mathbf{K}$. They are distinct and bi-orthogonal [33], [34]

$$ {}_L\langle j \mid j'\rangle_R = \delta_{jj'}. \tag{35}$$

If matrix $\mathbf{K}$ is simple, the eigenvectors are linearly independent and one obtains

$$\sum_j (|j\rangle_{RL}\langle j|) = \mathbf{I}. \tag{36}$$

This relation is equivalent to the closure relation with the Hermitian matrix. We conjecture that relation (36) holds for matrices involved in physical problems. The element $\langle \alpha n|\mathbf{G}(z)|\beta n'\rangle$ can be written [using (32) and (36)] as

$$\langle \alpha n|\mathbf{G}(z)|\beta n'\rangle = \sum_j \frac{\langle \alpha n \mid j\rangle_{RL}\langle j \mid \beta n'\rangle}{z-\eta_j} \tag{37}$$

which corresponds to the operator $\mathbf{G}(z)$ given by

$$\mathbf{G}(z) = \sum_j \frac{|j\rangle_{RL}\langle j|}{z-\eta_j}. \tag{38}$$

We want to determine this element (37) without having to compute the eigenvalues or eigenvectors of matrix $\mathbf{K}$. First, we introduce the following auxiliary function density:

$$g(x) = \sum_j \langle p \mid j\rangle_{RL}\langle j \mid q\rangle \delta(x-\eta'_j) \tag{39}$$

where $x = u, \eta'_j = \lambda_j$ with $m = 2$ or $x = \omega, \eta'_j = \mu'_j$ with $m = 1$. Vectors $|p\rangle$ and $|q\rangle$ are considered as data for the problem

$$|p\rangle = \sum_{\alpha n} p_\alpha(n)|\alpha n\rangle \quad \text{and} \quad |q\rangle = \sum_{\alpha n} q_\alpha(n)|\alpha n\rangle \tag{40}$$

$p_\alpha(n)(q_\alpha(n))$ are the Cartesian α components of $|p\rangle(|q\rangle)$ on the nth site. Now, we consider the function $R(z)$

$$R(z) = \int \frac{g(x)}{z+(-i)^m x}\,dx = \sum_j \frac{\langle p \mid j\rangle_{RL}\langle j \mid q\rangle}{z-\eta_j}. \tag{41}$$

It is clear that $R(z) = \langle \alpha n|\mathbf{G}(z)|\beta n'\rangle$ if $|p\rangle = |\alpha n\rangle$ and $|q\rangle = |\beta n'\rangle$. It is easy to show that, with the help of (33), (36), (38)

$$R(z) = \sum_{l=0}^{\infty} \frac{\mu_l}{z^{l+1}} \tag{42}$$

where μ_l represents the lth moment of $g(x)$ given by

$$\mu_l = \int g(x)x^l\,dx = \langle p|K^l|q\rangle \tag{43}$$

which can be directly computed from the known data $\mathbf{K}, |p\rangle$ and $|q\rangle$. Equation (42) is not convergent. However, it can be shown that if $|p\rangle = |q\rangle, R(z)$ can be developed in a continued convergent fraction

$$R(z) = \cfrac{b_0}{z-a_1-\cfrac{b_1}{z-a_2-\cfrac{b_2}{z-a_3-\cdots}}} \tag{44}$$

where the continued fraction coefficients are obtained by (with $s \geq 0$ and $b_0 = \nu_{00}$)

$$a_{s+1} = \frac{\bar{\nu}_{ss}}{\nu_{ss}} \tag{45}$$

and

$$b_{s+1} = \frac{\nu_{s+1\,s+1}}{\nu_{ss}} \tag{46}$$

with

$$\nu_{ss} = {}_L\langle t_s \mid t_s\rangle_R \tag{47}$$

and

$$\bar{\nu}_{ss} = {}_L\langle t_s|\mathbf{K}|t_s\rangle_R \tag{48}$$

ν_{ss} and $\bar{\nu}_{ss}$ are called the generalized moments. Vectors $|t_s\rangle_{R,L}$ are obtained by the following recursion:

$$|t_{s+1}\rangle_{R,L} = (K-a_{s+1})|t_s\rangle_{R,L} - b_s|t_{s-1}\rangle_{R,L} \tag{49}$$

starting with $|t_{-1}\rangle_{R,L} = 0$ and $|t_0\rangle_{R,L} = |p\rangle$. Nontrivial formulas (44)–(49) are well known in moments problem theory [35]. Equations (45)–(49) with the knowledge of data $\mathbf{K}$ and $|p\rangle\,(=|q\rangle)$, permit us to compute the coefficients a_s and b_s by iteration.

Our aim is to work with a large but finite-order matrix, so the number of eigenvalues is not infinite. In practice, we only calculate a few of the continued fraction coefficients. A test is inserted and the computation normally stops when b_s/b_{s-1} is smaller than 10^{-4}. If this value is quickly reached, the calculation stops and the results are considered exact. There are other strategies for problems with slow convergence [28]. Knowledge of (44) allows determination of Green functions of the system. The continued fraction is convergent and computation of coefficients a_s and b_s is stable if the density function $g(x)$ is a positive function. In the general situation, the positiveness of $g(x)$ is not rigorously established. However, in many physical problems it is shown (in the Appendix) that $g(x)$ is closely related to the energy dissipation (equal to zero if ε is zero) and is a positive function. When the matrix is symmetrical, the left and right eigenvectors are identical ($|j\rangle_R = |j\rangle_L$) and $g(x)$ is clearly positive.

Since development in the continued fraction is very stable and convergent with function $R(z)$ such that $g(x)$ given by (39) with $|p\rangle = |q\rangle$ is a positive function, it is very convenient to compute the nondiagonal term (37) as a linear combination of the $R(z)$ functions (44), with the form of the linear combination depending on the choice of $|q\rangle$ vectors. For instance, with a symmetrical real matrix we can choose

$$|p\rangle = |q\rangle = |\alpha n\rangle + |\beta n'\rangle \tag{50}$$

obtaining $R^+(z)$ and

$$|p\rangle = |q\rangle = |\alpha n\rangle - |\beta n'\rangle \tag{51}$$

obtaining $R^-(z)$, then the Green function is given by

$$\langle \alpha n|\mathbf{G}(z)|\beta n'\rangle = \frac{(R^+(z)-R^-(z))}{4} \tag{52}$$

with a matrix having complex eigenvectors, the choice of the $|p\rangle$ and $|q\rangle$ vectors can be more complex [20].

B. Computing Aspects

Let us now consider how the dynamical matrices are obtained. With the potential vector, the matrix $\mathbf{D}$ is given by (11). With the electromagnetic field, after discretization of the motion equations (17) and (18), the local physical properties of a point n of the media is represented by six small interaction matrices $\mathbf{m}$ of (6 × 6) dimension. Indeed, in 3-D space, there is one matrix $\mathbf{m}$ for every bound between site n and the six neighboring sites n'. These matrices $\mathbf{m}$ can be expressed schematically as with $\mathbf{N} = (\varepsilon)^{\frac{1}{2}}$

$$\mathbf{m} = \begin{pmatrix} 0 & \mathbf{N}^{-1}\mathbf{R} \\ \mathbf{R}\mathbf{N}^{-1} & 0 \end{pmatrix} \tag{53}$$

where $\mathbf{N}^{-1}\mathbf{R}$ and $\mathbf{R}\mathbf{N}^{-1}$ arise, respectively, from the discretization of (17) and (18). Spatial derivatives in $\mathbf{R}\mathbf{N}^{-1}$ take into account the heterogeneity of the media. $\mathbf{R}$ is a (3 × 3) matrix corresponding to the discretized rotational operator. Index matrices $\mathbf{N}$ of dimension (3 × 3) represent the local electromagnetic properties of the medium expressed in the laboratory frame. Schematically, with the electromagnetic field, the system can be seen as a cubic lattice of "particles" of mass $\varepsilon(n)$, every particle having six degrees of freedom. Interactions are between the particle and its first neighbors only and can be represented by "spring" (every "spring" has been characterized by a (6 × 6) elastic tensor). In this scheme, current source at site n is equivalent to a "force" applied to the nth particle. Response at site m are given by the "displacement" of the mth particle.

In practice, first we compute the dynamical matrix $\mathbf{M}$ (or $\mathbf{D}$) of the medium under consideration. This matrix is sparse and we use special method of storage. Now we assume that we have a source at site n', polarized along the β axis and we want to compute the α component of electric field created by this source at site n. Then the $6N$ components of the vector $|p\rangle = |t_0\rangle$ are equal to zero unless for the αn and $\beta n'$ components, which are set to one. Coefficients of the continued fraction (44) $R^+(z)$ are obtained from the iterations shown at the bottom of the page.

$R^-(z)$ is obtained starting from $|p\rangle = |t_0\rangle$ where $\alpha n'$ component equal to one and βn component is equal to -1. Green function is obtained from (52).

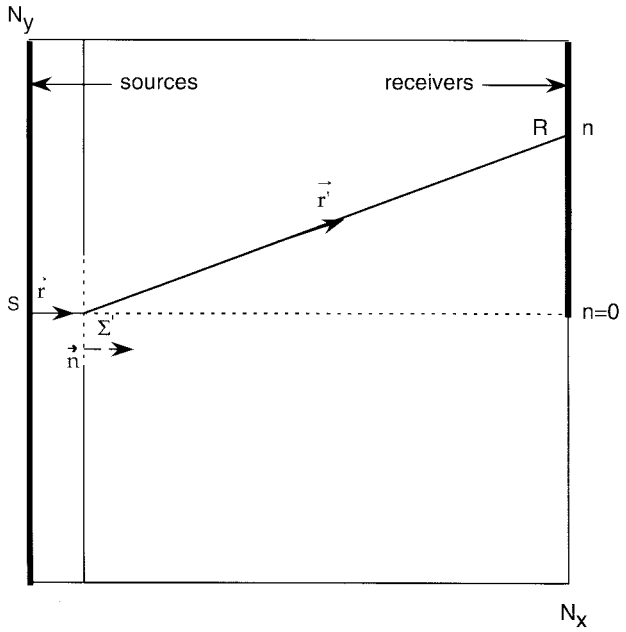

Fig. 1. The 2-D model: dimension of the box $N_x = N_y = 301$, position of the screen $= 30$, width of the aperture $= 60$. The incident plane wave is simulated by introducing a uniform current density in the (yoz) plane polarized parallel to the z axis. (o = sources, x = receivers.)

To simulate a plane electromagnetic wave propagating in the x-axis direction (Fig. 1) with the electric field polarized following a direction P in the y-z plane, we introduce, in this plane, a uniform current density parallel to the P axis. It can be easily shown that such a source is equivalent to a point source at infinity in the direction perpendicular to the yz plane. The receiver is located on the opposite side of the sample. Periodic boundary conditions are taken along the y direction (2-D) or along the y and z directions (3-D).

IV. Applications: Diffraction by a Rectangular Aperture

In order to test our method, we have computed the electromagnetic field diffracted by a slit (2-D media) and a rectangular aperture (3-D media) and we have compared the computed values to the results of Kirchhoff's diffraction

$$|\mathbf{t}_0\rangle$$

$$\nu_{00} = \langle \mathbf{t}_0 \mid \mathbf{t}_0 \rangle \qquad \bar{\nu}_{00} = \langle \mathbf{t}_0 | \mathbf{M} | \mathbf{t}_0 \rangle$$

$$\mathbf{a}_1 = \frac{\bar{\nu}_{00}}{\nu_{00}}$$

$$|\mathbf{t}_1\rangle = \mathbf{M}|\mathbf{t}_0\rangle - \mathbf{a}_1|\mathbf{t}_0\rangle$$

$$\nu_{11} = \langle \mathbf{t}_1 | \mathbf{t}_1 \rangle \qquad \bar{\nu}_{11} = \langle \mathbf{t}_1 | \mathbf{M} | \mathbf{t}_1 \rangle$$

$$\mathbf{a}_2 = \nu_{11\nu_{11}}, \mathbf{b}_1 = \frac{\nu_{11}}{\nu_{00}}$$

$$|\mathbf{t}_2\rangle = \mathbf{M}|\mathbf{t}_1\rangle - \mathbf{a}_2|\mathbf{t}_1\rangle - \mathbf{b}_1|\mathbf{t}_0\rangle.$$

theory. The computations were performed on an IBM SP2 computer.

To simulate our system, we consider a parallelepiped box of size $L_x * L_y * L_z$, which is discretized by the $N_x * N_y * N_z$ lattice (N_x, N_y, N_z are integers). The grid spacings $\Delta x, \Delta y$ and Δz are determined through the relations $L_x = N_x * \Delta x, L_y = N_y * \Delta y$ and $L_z = N_z * \Delta z$. We assume that the electromagnetic plane waves propagate along the x axis and that the electric field is polarized in the z direction. To simulate the plane wave, we introduce, in the (yoz) plane, a uniform current density parallel to the z axis. The receivers are located on the opposite face of the grid. Periodic boundary conditions are assumed in the y direction with the slit and y and z directions with the rectangular aperture. With these boundary conditions, our system is equivalent to a diffraction grating. We do not introduce any absorbing conditions at the limit of the box.

To work with very large systems, i.e., with a high-order matrix (about several millions), it is necessary to develop new storage techniques. The method we used involved considering the matrix as a system of sites, interacting with neighboring sites only through a local interacting matrix. So, we only store the different values of these local matrices and, for every site, the type and number of neighboring sites. When we solve Maxwell equations directly in terms of $\vec{E}$ and $\vec{B}$, the elementary interaction matrices are $(6 * 6)$ anti-symmetrical matrices. To resolve the equations using vector potential, for isotropic media, local matrices are reduced to scalars.

We verify the accuracy of the SMM results by comparing them to those obtained by the theoretical solution given by the Kirchhoff approximation formula [36]

$$I(r) \sim \left| \int \frac{[\cos(\vec{n}, \vec{r}') - \cos(\vec{n}, \vec{r})]}{|\vec{r} - \vec{r}'|} e^{-ik|\vec{r}-\vec{r}'|} \, d\Sigma' \right|^2 \quad (54)$$

where $\vec{\mathbf{n}}$ is a unit vector normal to Σ' and pointing to diffraction region (see Fig. 1). The Kirchhoff approximation supposes that the frequency of the incident wave is not too small (wide-wavelength limits) and not too high (narrow-wavelength limits). In our computation, we work at frequencies such as $\lambda \sim l$, where l is the linear size of the aperture and $\lambda > 10$–$20\Delta x$ with $\Delta x = \Delta y = \Delta z$ being the parameters of the grid. The periodic boundary conditions are taken into account in the calculation of the Kirchhoff integral. Absorption coefficient was also included in the Kirchhoff formula where the wave vector was considered complex. In the following, the frequencies are given in reduced units. To obtain the frequency in hertz, it is necessary to multiply the value given in reduced units by three $10^8 \frac{1}{\Delta x}$ (with $\Delta x = \Delta y = \Delta z$ given in meters).

A. Diffraction of Plane Electromagnetic Waves by a Slit

There is no variation in the field quantities with respect to z Cartesian coordinates. Our system is illustrated in Fig. 1. For this case, we choose $N_x = 301, N_y = 301$. In the nodes range $I = N_x/10$, we consider a screen characterized by a high refractive index ($\varepsilon_2 = 10^6$) with an aperture size of 20% N_y.

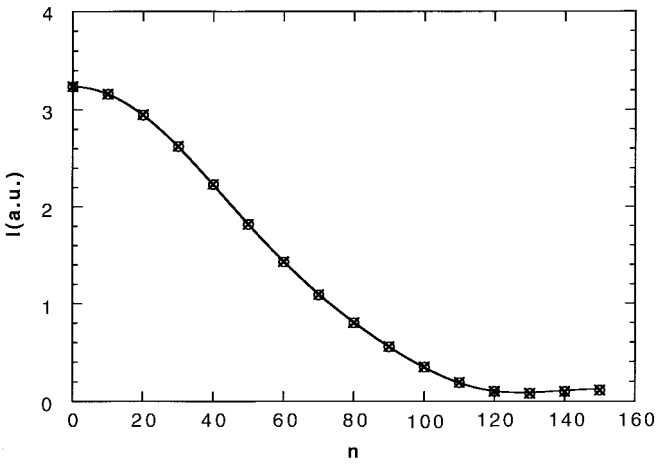

Fig. 2. Computation of the intensity diffracted by a slit for frequency $\omega = 0.1$ and $\varepsilon = 0.05$ versus receiver positions n. The origin $n = 0$ is taken at the center of the edge $I = N_x$, **O** vector potential, **X** electric field, analytical values.

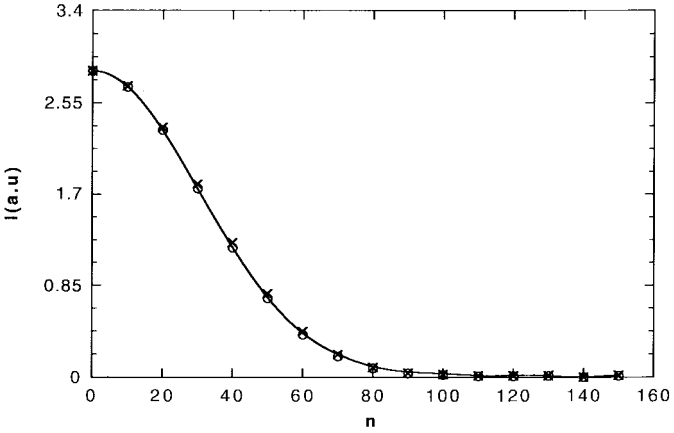

Fig. 3. Computation of the intensity diffracted by a slit for frequency $\omega = 0.3$ and $\varepsilon = 0.05$ versus receiver positions n. The origin $n = 0$ is taken at the center of the edge $I = N_x$, **O** vector potential, **X** electric field, analytical values.

1) Vector Potential Results: The Green function of the system is obtained from the difference between $R^+(z)$ and $R^-(z)$. To compute the Green function, we have used 450 generalized moments. It is very important to note the exceptional stability of the method. The differences $a_s^+ - a_s^-$ and $b_s^+ - b_s^-$ are null until the 200 range. Thus, if we stop computation of the continued fractions before this value, the difference between $R^+(z)$ and $R^-(z)$ will be equal to zero. This means that coefficients a_s and b_s have a physical meaning for large s, even up to 450. The SMM gives the response for all frequencies between zero and $\omega_{\max}$ where $\omega_{\max}$ depends on the discretization scheme. Here, we present results only for some specific values of the frequency. The behavior of the modulus squared of the vector potential obtained by SMM versus the receiver positions are shown for frequencies: $\omega = 0.1$ with $\varepsilon = 0.05$ in Fig. 2, $\omega = 0.3$ with $\varepsilon = 0.05$ in Fig. 3, $\omega = 0.1$ with $\varepsilon = 0.005$ in Fig. 4, and $\omega = 0.3$ with $\varepsilon = 0.005$ in Fig. 5. In these figures, we also provide the analytical results obtained with the Kirchhoff formula. The two results are clearly in very good agreement.

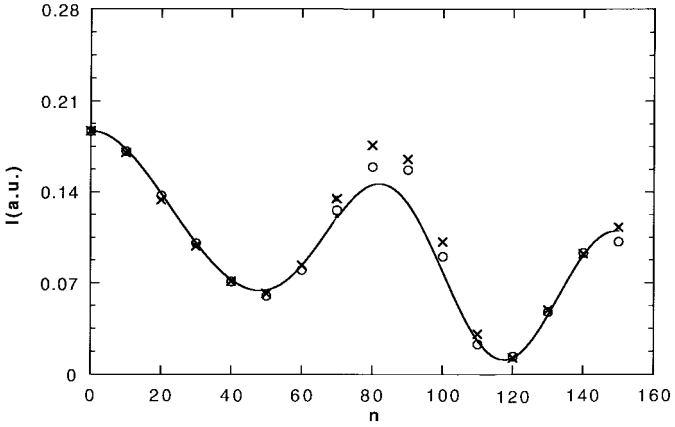

Fig. 4. Computation of the intensity diffracted by a slit for frequency $\omega = 0.1$ and $\varepsilon = 0.005$ versus receiver positions n. The origin $n = 0$ is taken at the center of the edge $I = N_x$, **O** vector potential, **X** electric field, analytical values.

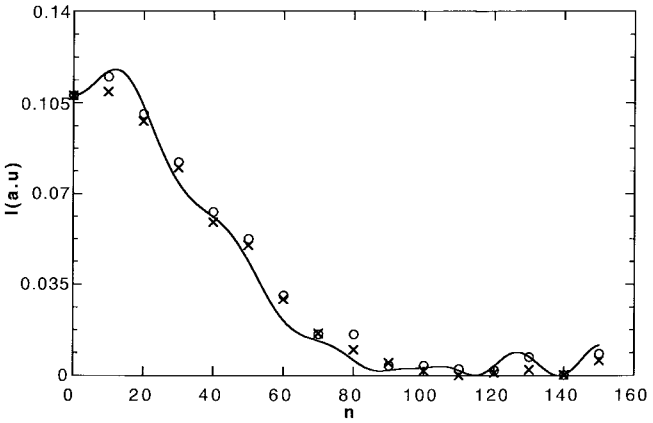

Fig. 5. Computation of the intensity diffracted by a slit for frequency $\omega = 0.3$ and $\varepsilon = 0.005$ versus receiver positions n. The origin $n = 0$ is taken at the center of the edge $I = N_x$, **O** vector potential, **X** electric field, analytical values.

2) Electromagnetic Field Results: Similarly, we have studied the diffraction of electromagnetic plane wave propagation in a 2-D isotropic medium by an aperture using the motion equation (19). We consider a lattice identical to that used in the $\vec{A}$ study. We calculated 600 moments. In Figs. 2–5, we also give the modulus squared of the electric field obtained by SMM versus the receiver positions for the same frequency and damping values, compared to previous results. We see that there is excellent agreement with the results obtained analytically and those obtained from the potential vector.

B. Diffraction by a Rectangular Aperture

In the following, we have easily extend SMM to compute Green functions in 3-D space. To illustrate the problem, we only present results obtained with the potential vector.

The calculation uses a $(101 * 101 * 101)$ grid $(N_x = N_y = N_z = 101)$, which corresponds to $(1\,030\,301 \times 1\,030\,301)$ matrix. Here we solve vector potential (9). The opening is a square with side $a = 20\%N_y$ placed in the plane (yoz) at $I = N_{x/10}$. We calculated 500 moments.

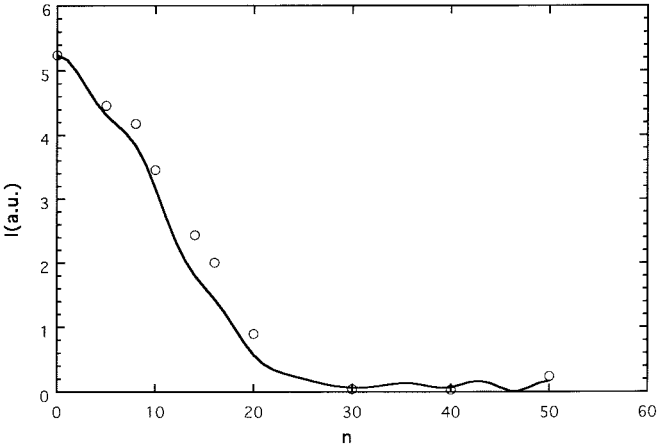

Fig. 6. Computation of the intensity diffracted by a rectangular aperture for frequency $\omega = 1$ and $\varepsilon = 0.05$ versus receiver positions n. The origin $n = 0$ is taken at the center of the face $I = N_x$, **O** vector potential, analytical values.

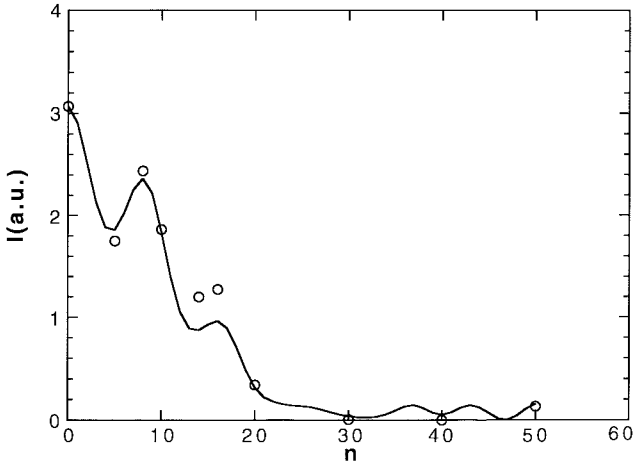

Fig. 7. Computation of the intensity diffracted by a rectangular aperture for frequency $\omega = 1$ and $\varepsilon = 0.005$ versus receiver positions n. The origin $n = 0$ is taken at the center of the face $I = N_x$, **O** vector potential, analytical values.

We present the results calculated by SMM and those obtained analytically with the Kirchhoff approximation formula for frequency $\omega = 1$ with $\varepsilon = 0.05$ in Fig. 6 and $\omega = 1$ with $\varepsilon = 0.005$ in Fig. 7. There is excellent agreement between theses results.

V. Discussion and Conclusion

In this work, we have reported two types of results: one uses the potential vector and the other uses the $(\vec{E}, \vec{B})$ field. Both approaches give very good results. With the potential vector $\vec{A}$, matrix dimensions are smaller than with the $(\vec{E}, \vec{B})$ field and the CPU time taken by the computer program was lower (with $\vec{A}$ the CPU time is 0.24 s per moment and with $(\vec{E}, \vec{B})$ it is 1.22 s per moment for 2-D system). This permits us to work more easily with larger systems, e.g., in three dimensions. However, in anisotropic or heterogeneous media when using the $(\vec{E}, \vec{B})$ field, the matrices are strictly antisymmetrical (these matrices can be easily transformed into symmetrical matrices), which is a great advantage when using SMM. With the potential vector,

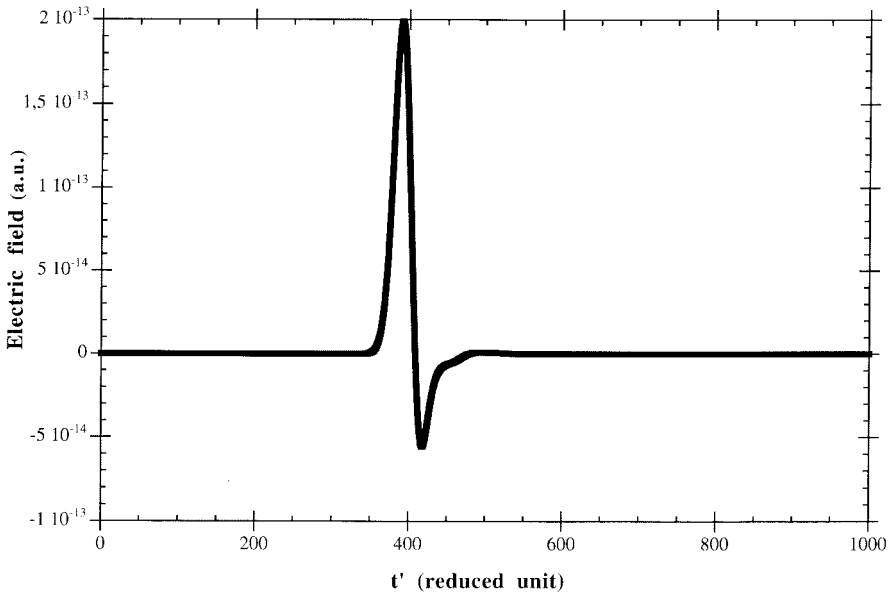

Fig. 8. Variations in the electric field over time at the center of the face $I = N_x$ with $\varepsilon = 0.05$. A source pulse is applied at time $t'_0 = 100$ in the yoz plane.

the matrices are not always symmetrical. Consequently, the use of either method depends on the problem that has to be solved.

The second point concerns the absorption boundary conditions. We did not insert any such conditions here. How can the good results be explained? In SMM, we compute the Green function between source points on the yoz surface at $x = 0$ and a point (receiver) in the yoz surface at $x = L_x$.

The Green function $\langle R|G(t-t')|S\rangle$ represents the response of the receiver R at time t when a pulse (Dirac) has been applied at the source S at time t'. This Green function can be computed by taking the inverse Fourier transform of $\langle R|G(\omega)|S\rangle$. Applying a pulse at time t' in the yoz surface will produce a electromagnetic wave that, in the absence of absorption in the box, will propagate from one side to other side indefinitely. Thus, computation of the electromagnetic field in the yoz plane at $x = L_x$ will include this effect and the results will not be in agreement with the Kirchhoff theory. With the finite-difference method, one usually introduces absorbing boundary conditions [2]–[4]. However, in SMM, coefficient ε represents energy dissipation (finite lifetime of photons), so it is possible to choose this coefficient so that only one wave arrives on the opposite site of the box and other reflections are weak or eliminated. To illustrate this effect, we computed the time dependence of the electric field in a receiver at the center of the arrival face when a Gaussian source is applied in the source plane at time $t'_0 = 100$. Figs. 8 and 9 show variations in the electric fields with $\varepsilon = 5\,10^{-2}$ and $\varepsilon = 5\,10^{-3}$, respectively. It is clear that with $\varepsilon = 5\,10^{-2}$, only one wave reaches the receiver, while with $\varepsilon = 5\,10^{-3}$, several waves reach the receiver. However, even with $\varepsilon = 5\,10^{-3}$, the form of the diffracted pattern is in good agreement with the analytical results, showing that the contribution of the secondary waves is weak. The form of the wave with $\varepsilon = 5\,10^{-2}$ is in agreement with the response of a 2-D media where the Green functions are Hankel functions (in free-space). It is easy to verify that results obtained with $\varepsilon = 5\,10^{-3}$ do not markedly differ from those obtained with nonabsorbing media ($\varepsilon = 0$) and represent a good approximation of free media. Now, we compare SMM with other computing methods.

It is difficult to make comparisons with the usual moment methods [5]. In this latter method, only the diffracting object is discretized and free-space Green functions are used to compute the diffracted field. In the usual moment methods, it is necessary to invert full matrices limiting the size of the diffracting object. Diffraction is also computed for a given frequency. In SMM, all space is discretized and the exact Green functions are computed for all frequencies.

There has been only one comparison until now, in electromagnetism, with the finite-difference method [37]. However, the results obtained in the simulation of acoustic wave propagation [29] provide some general information about both methods. The same conclusions will be certainly true for the simulation of electromagnetic wave propagation. In the finite-difference method, values for the fields are obtained for every point of the space, while with SMM computation of the fields is performed separately for each point. This is a substantial disadvantage of SMM in some applications. Use of large parallel processing will certainly allow us to improve the performance of SMM. The computing time for the determination of n generalized moments is about the same as that necessary to compute n steps with the finite-difference method. In SMM, one works indirectly with the whole set of eigenvalues and eigenvectors of matrices $\mathbf{D}$ or $\mathbf{K}$. So, the results are not very sensitive to the details of discretization processes. For instance, it is not necessary to take into account very precise boundary conditions at the corners of the box in 2-D media or edges of the box in 3-D media. Simple discretization schemes work very well. We think that this effect arises because time is not discretized in SMM. Furthermore, with SMM, knowledge of the Green functions allows one to compute the response regardless of the form of the source,

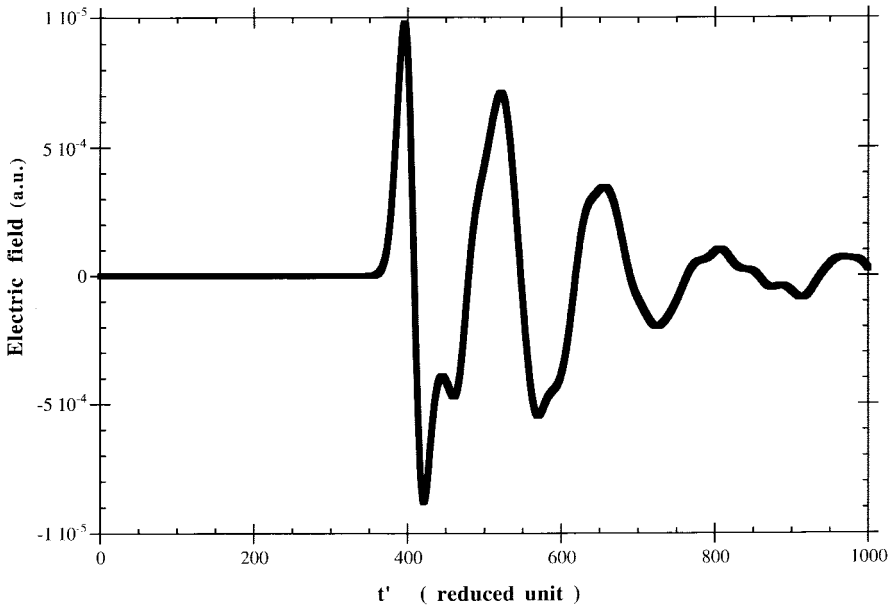

Fig. 9. Variations in the electric field over time at the center of the face $I = N_x$ with $\varepsilon = 0.005$. A source pulse is applied at time $t'_0 = 100$ in the yoz plane.

while with the finite-difference method it is necessary to make a run for every type of source.

In conclusion, we have presented simulations of electromagnetic waves propagating in 2-D and 3-D media using SMM, thus introducing a new approach for numerical resolution of wave propagation problems. The method can be used regardless of the number, nature, or form of the diffracting objects. Comparison between the analytical solutions and the spectral moments-method results proves the accuracy of this method. Applications to the computation of radar cross sections and propagation in anisotropic heterogeneous media (such as liquid crystals [38]) are now being developed.

APPENDIX

Here we show that function $g(x)$ given by (39) (with $|p\rangle = |q\rangle$) is always a positive (or semi-positive) function even with nonsymmetrical matrix. To illustrate this situation with $(\vec{E}, \vec{B})$ fields, let us consider a volume V and a discrete set of point charges q_n located at the points $\vec{\mathbf{r}}_n$ inside V. The power of the electromagnetic field converted into thermal energy (Joule effect) is given by Jackson [31]

$$W = \int \vec{J}_0(\vec{r}, t) \cdot \vec{E}(\vec{r}, t)\, dv \tag{A.1}$$

with

$$\vec{J}_0(\vec{r}, t) = \sum q_n \vec{v}_n(t) \delta(\vec{r} - \vec{r}_n(t)). \tag{A.2}$$

Now, with complex harmonic fields, the average dissipated energy is given by

$$\bar{W} = \frac{1}{2} RP \int \vec{J}_0^*(\vec{r}) \cdot \vec{E}(\vec{r})\, d^3v. \tag{A.3}$$

In site representation (A.3) can be written as

$$\bar{W} = \frac{\Delta V}{2} RP \sum_{\alpha n} J^*_{0\alpha}(n) E_\alpha(n) = \frac{\Delta V}{2} RP \langle J_0 \mid E \rangle \tag{A.4}$$

where ΔV is the volume element.

From (27), we know that with the electromagnetic field $(\vec{E}, \vec{B})$

$$|\Phi(\omega)\rangle = \mathbf{G}(\omega)|J'(\omega)\rangle \tag{A.5}$$

and considering only the electric components, one obtains from (15) and (27)

$$|E'(\omega)\rangle = [\varepsilon_r]^{\frac{1}{2}} |E(\omega)\rangle = \mathbf{G}(\omega)|J'(\omega)\rangle \tag{A.6}$$

so that using (17)

$$\bar{W} = \frac{\Delta V}{2c\mu_0} RP \langle J'(\omega)|\mathbf{G}(\omega)|J'(\omega)\rangle. \tag{A.7}$$

Taking into account the form of the Green operator (31) with the $(\vec{E}, \vec{B})$ field and $z = i(\omega + i\varepsilon)$, in the limit $\varepsilon \to 0+$ one obtains

$$\begin{aligned}
\bar{W} &= -\frac{\Delta V}{2c\mu_0} RP \left[i \sum_j \frac{\langle J' \mid j \rangle_{RL} \langle j \mid J' \rangle}{\omega + i\varepsilon - \mu'_j} \right] \\
&= -\frac{\Delta V}{2c\mu_0} RP \left[\sum_j \frac{\langle J' \mid j \rangle_{RL} \langle j \mid J' \rangle \varepsilon}{(\omega - \mu'_j)^2 + \varepsilon^2} \right. \\
&\quad \left. + i \sum_j \frac{\langle J' \mid j \rangle_{RL} \langle j \mid J' \rangle (\omega - \mu'_j)}{(\omega - \mu'_j)^2 + \varepsilon^2} \right] \\
&= -\frac{\pi}{2} \frac{\Delta V}{c\mu_0} \sum_j \langle J' \mid j \rangle_{RL} \langle j \mid J' \rangle \delta(\omega - \mu'_j).
\end{aligned} \tag{A.8}$$

$\bar{W}$ is the energy loss by the electromagnetic field and must be a negative function [32]. So the function

$$g(\omega) = \sum_j \langle J' \mid j \rangle_{RL} \langle j \mid J' \rangle \delta(\omega - \mu'_j) \tag{A.9}$$

must be a positive function regardless of the values of charges q_n in (A.2). Expression (A.9) has exactly the same form as (39) with $|p\rangle = |q\rangle$. The same result could be obtained using the potential vector.

REFERENCES

[1] A. Taflove and Umashankar, "Finite element and finite difference methods in electromagnetic scattering," in *Pier 2*, M. A. Morgan, Ed. Amsterdam, The Netherlands: Elsevier, 1990, ch. 8.

[2] G. Mur, "Absorbing boundary conditions for the finite-difference approximations of the time-domain electromagnetic field equations," *IEEE Trans. Electromagn. Compat.*, vol. EMC-23, pp. 377–382, Nov. 1981.

[3] J. P. Berenger, "A perfectly matched layer for absorption of electromagnetic wave," *J. Comput. Phys.*, vol. 114, no. 12, pp. 185–200, Oct. 1994.

[4] D. S. Katz, E. T. Thiele, and A. Taflove, "Validation and extention to three dimensions of the Berenger PML absorbing boundary condition for FD-TD meshes," *IEEE Microwave Guided Wave Lett.*, vol. 10, pp. 268–270, Aug. 1994.

[5] R. F. Harrington, *Field Computation by Moment Methods*. New York: Macmillan, 1968.

[6] S. M. Rao, D. R. Wilton, and A. W. Glisson, "Electromagnetic scattering by surfaces of arbitrary shape," *IEEE Trans. Antennas Propagat.*, vol. AP-30, pp. 409–418, May 1982.

[7] E. W. Montroll, "Frequency spectrum of crystalline solids," *J. Chem. Phys.*, vol. 10, pp. 218–229, 1942.

[8] C. Blumstein and J. C. Wheeler, "Modified-moments method: Application to harmonic solids," *Phys. Rev. B.*, vol. 8, no. 4, pp. 1764–1776, Aug. 1973.

[9] J. C. Wheeler, M. G. Prais, and C. Blumstein, "Analysis of spectral density using the modified moments," *Phys. Rev. B*, vol. 10, no. 6, pp. 2429–2447, Sept. 1974.

[10] C. Benoit, "An analysis of the frequency distribution function and dielectric and scattering properties, using the orthogonalised-moments method," *J. Phys. C: Solid State Phys.*, vol. 20, no. 6, pp. 765–789, Feb. 1987.

[11] ———, "Determination of the inelastic neutron scattering cross section by the spectral moments method: Application to incommensurate crystal and quasi-crystal," *J. Phys. Condens. Matter*, vol. 1, no. 2, pp. 335–345, Jan. 1989.

[12] C. Benoit, G. Poussigue, and A. Assaf, "Dynamic and scattering properties of the Sierpinski gasket," *J. Phys. Condens. Matter*, vol. 4, no. 12, pp. 3153–3177, Mar. 1992.

[13] E. Royer, C. Benoit, and G. Poussigue, "Numerical study of dynamical properties of very large percolating cluster in d-dimensions ($2 \leq d \leq 6$)," in *High Performance Computing II*, M. Durand and F. El Dabaghi, Eds. North Holland, The Netherlands: Elsevier, 1991, pp. 513–524.

[14] ———, "Dynamic of percolating networks," *J. Phys. Condens. Matter*, vol. 4, no. 2, pp. 561–569, Jan. 1992.

[15] A. Rahmani, C. Benoit, E. Royer-Vilanova, and G. Poussigue, "Vibrational properties of random percolating networks," *J. Phys. Condens. Matter*, vol. 5, no. 43, pp. 7941–7954, Oct. 1993.

[16] A. Rahmani, C. Benoit, and G. Poussigue, "A fractal model for silica aerogels," *J. Phys. Condens. Matter*, vol. 6, no. 8, pp. 1483–1496, Feb. 1994.

[17] G. Poussigue, C. Benoit, J. L. Sauvajol, J. P. Lere-Porte, and C. Chorro, "Dynamics of polythiophene with defects," *J. Phys. Condens. Matter*, vol. 3, no. 45, pp. 8803–8824, Nov. 1991.

[18] C. Benoit, G. Poussigue, and A. Azougarh, "Neutron scattering by phonons in quasicrystal," *J. Phys. Condens. Matter*, vol. 2, no. 11, pp. 2519–2536, Mar. 1990.

[19] G. Poussigue, C. Benoit, M. de Boissieu, and R. Currat, "Inelastic neutron scattering by quasicrystals: A model for icosahedral Al-Mn; for Al-Mn-Pd comparison with the experimental results," *J. Phys. Condens. Matter*, vol. 6, no. 3, pp. 659–678, Jan. 1994.

[20] C. Benoit, "The moments method and damped systems," *J. Phys. Condens. Matter*, vol. 6, no. 17, pp. 3137–3160, Jan. 1994.

[21] J. P. Gaspard and F. Cyrot-Lackmann, "Density of states from moments. Application to the impurity band," *J. Phys. C: Solid-State Phys.*, vol. 6, no. 21, pp. 3077–3093, Oct. 1973.

[22] P. Lambin and J. P. Gaspard, "Continued-fraction technique for tight-binding systems: A generalized-moments method," *Phys. Rev. B*, vol. 26, no. 8, pp. 4356–4368, Oct. 1982.

[23] P. Turchi, F. Ducastelle, and G. Treglia, "Band gaps and asymptotic behavior of continued fraction coefficients," *J. Phys. C: Solid-State Phys.*, vol. 15, no. 13, pp. 2891–2924, May 1982.

[24] E. Jurczek, "Orthogonalized-moments method," *Phys. Rev. B*, vol. 32, no. 6, pp. 4208–4211, Sept. 1985.

[25] C. Lanczos, "An iteration method for the solution of the eigenvalue problem of linear differential and integral operators," *J. Res. Nat. Bur. Stand.*, vol. 45, pp. 255–282, 1950.

[26] R. Haydock, "The recursive solution of the Schrödinger equation," in *Solid-State Phys.*, H. Ehrenreich, F. Seitz, and D. Turnbull, Eds. London, U.K.: Academic, 1980, vol. 35, pp. 216–294.

[27] C. Benoit, E. Royer, and G. Poussigue, "The spectral moments method," *J. Phys.: Condens. Matter*, vol. 4, no. 12, pp. 3125–3152, Mar. 1992.

[28] T. J. Stieltjes, "Quelques recherches sur la theorie des quadratures dites mécaniques," *Ann. Ecole Normale*, 3° serie Tome 1, pp. 409–460, 1884.

[29] V. Rousseau, C. Benoit, R. Bayer, M. Cuer, and G. Poussigue, "Elastic wave-propagation simulation in heterogeneous media by the spectral moments method," *Geophys.*, vol. 61, no. 5, pp. 1269–1281, Sept. 1996.

[30] C. Benoit, G. Poussigue, V. Rousseau, Z. Lakhliai, and D. Chenouni, "Determination of the Green functions with large nonsymmetric matrices by moments method," *Modeling Simul. Mater. Sci. Eng.*, vol. 3, pp. 161–185, Apr. 1995.

[31] J. D. Jackson, *Classical Electrodynamics*. New York: Wiley, 1962.

[32] E. Royer, "Etude numerique de la méthode des moments spectraux et application aux reseaux de percolation," Ph.D. dissertation, Univ. Montpellier, France, 1992.

[33] F. R. Gantmacher, *Theorie des Matrices*, J. Gabay, Ed. Paris, France: Dunod, 1966.

[34] E. Isaacson and H. B. Keller, *Analysis of Numerical Methods*. New York: Wiley, 1966.

[35] N. Akhieser, *The Classical Moment Problem*. Edinburg, U.K.: Oliver-Boyd, 1965.

[36] M. Born and E. Wolf, *Principales of Optics*. Oxford, U.K.: Pergamon, 1956.

[37] G. Poussigue, C. Benoit, D. Chenouni, and Z. Lakhliai, "Détermination par la méthode des moments spectraux de la diffraction des ondes électromagnétiques par un cylindre diélectrique de section circulaire ou carrée," *C. R. Acad. Sci. Paris*, t. 322, Série II.b, pp. 733–740, May 1996.

[38] Z. Lakhliai, D. Chenouni, C. Benoit, G. Poussigue, M. Brunet, S. Quentel, and A. Sakout, "Numerical study of electromagnetic wave propagation in twisted birefringent layers by the spectral moments method," *Modeling Simul. Mater. Eng.*, vol. 4, pp. 597–611, Dec. 1996.

Driss Chenouni received the Ph.D. degree in physics from the University of Montpellier II, France, in 1989, and the State Doctors' degree from the University of Fes, Morocco, in 1996.

He is currently a Professor of physics at the University of Fes, Morocco. His original research concerned the raman scattering of light in conducting polymers. Since 1992 he has been working on applications of the spectral moments method to simulate electromagnetic waves diffraction in heterogeneous media.

Zakia Lakhliai received the Ph.D. degree in physics from the University of Montpellier II, France, in 1987, and the State Doctors's degree from the University of Fes, Morocco, in 1996.

She is currently a Professor of physics at the Fes Institute of Technology, Morocco. Her original research concerned the optical properties of conducting polymers. Since 1992 she has been working on applications of the spectral moments method to simulate the propagation of electromagnetic waves in anisotropic media.

Claude Benoit received the State Doctor's degree from Montpellier University, France, in 1969.

He joined the Montpellier faculty in 1974 and is currently a Professor. His research primarily involves the dynamics of crystal lattice, infrared absorption, Raman scattering of light, and inelastic scattering of neutrons. He has been developing the spectral moments method since 1987 and has been working on applications of this method to simulate acoustic and electromagnetic wave propagation since 1992.

Gérard Poussigue received the Licence ès Sciences degree from Nancy University, France, in 1961, the Engineer Diploma degree from Ecole National Superieure de Industries Chimiques, Nancy, France, in 1962, and the State Doctor's degree (molecular physics research) from Paris VI University, France, 1968.

Since 1969, he has been a Researcher at Centre National de la Recherche Scientifique, Paris, France. In 1987 he worked at Montpellier II University in the field of solid physics. Among his research interest are the application of the Benoit's spectral moments method to various macroscopic problems such as solid-state dynamics, electromagnetism, and geophysics.

Abdallah Sakout received the Ph.D. degree in electronics from the University of Montpellier II, France, in 1983, and the State Doctors's degree from the University of Lyon I, France, in 1987.

He is currently a Professor of Physics in the University of Fes, Morocco. His original research concerned the modelization of thermal transferts under laser illumination. Since 1992 he has been working on applications of the spectral moments method in solid state and electromagnetism.